AlGaN/GaN Power FET

by Seikoh Yoshida *

ABSTRACT GaN and related compound semiconductors, as well as SiC and diamond, are wide bandgap semiconductors that also have high melting points, and high electric breakdown fields. These materials therefore have potential for the power electronic devices that can be operated under conditions of high breakdown voltage, high frequency, and high temperature. In Japan, the development of GaN has progressed to fabricate blue light emitting diodes (LED) and laser diodes (LD). In the U.S.A., research on GaN electronic devices has already begun. However, recently in Japan, research on GaN electronic devices for high-frequency applications started with the 673 K operation GaN metal semiconductor field effect transistor (MESFET) presented by the Furukawa Electric Co. In this research, we paid attention to the excellent figures of merit of GaN, which can be operated under conditions of high current and high breakdown voltage, and successfully performed high-current operation (20 A) of an AlGaN/GaN hetero FET for the first time. The minimum on-state resistance (R_{on}) was 2 mΩcm^2 at 100 V. This is the lowest value for a GaN-based FET, and corresponds to one-quarter of that of Si-devices.

1. INTRODUCTION

In the 21st century, environmental measures such as reducing CO_2 emissions have been demanded in energy development. Si switching devices are generally used as electric power converting devices. To reduce power loss, the density of Si device integration has become satisfactorily high. As a result, the on-state resistance of a Si metal oxide semiconductor field effect transistor (MOSFET) reached the theoretical limit of Si. On the other hand, wide bandgap semiconductors such as SiC, GaN, and diamond also have a wide bandgap, small atomic binding distance, large binding energy (strong for radiation damage), and thermal stability. They therefore have great potential as hard electronic materials which exceed Si [1].

Suitable material properties for a hard electronic material include breakdown electric field, saturation velocity, thermal conductivity, mobility, and dielectric constant. Figures of merit [2~6] combined with these material properties for high power, high speed, high frequency, and low loss have already been reported. GaN also has excellent figures of merit compared with those of Si and GaAs [7].

In particular, it should be noted that the on-state resistance of GaN FET can be remarkably reduced to less than that of Si MOSFET by a two or three order of magnitude, and GaN FET has potential for low-loss and cooling free power switching devices and inverters, which are difficult to realize using Si devices. The uses of high-temperature devices are high-temperature sensor, aircraft, space rocket engine controller, atomic energy equipment, and measuring instruments for underground exploration. The good features of high-temperature operation devices are that they do not require a large cooling system to suppress heat (or the cooling system is very small).

Recently, GaN electronic devices have been actively developed in the U.S.A. Also in the U.S.A., several venture companies selling and manufacturing GaN electronic devices have recently been established. Furthermore, Air Force and Naval Research have also been actively researching military applications. Other uses of GaN electronic devices are electric power switching devices such as inverters, converters, relay switching devices, and high-frequency devices.

Among high-temperature operation devices, metal semiconductor field effect transistors (MESFET) [8~10], hetero field effect transistors (HFET) [11], and modulation doped field effect transistors (MODFET) [12] have already been reported. Not only in the U.S.A. but also in Japan, high-frequency devices such as high electron mobility transistors (HEMT) and HFET using an AlGaN/GaN heterostructure and two-dimensional electron gas (2DEG) have been developed, and the maximum frequency for operation is over 130 GHz. This report describes the fabrication of AlGaN/GaN power HFET and how we obtained a very low on-state resistance (2 mΩcm^2) with a value that corresponds to one-quarter of that of Si MOSFET. Furthermore, it is reported that AlGaN/GaN HFET was operated under conditions of 20 A, and the maximum Schottky breakdown voltage of gate and source was 600 V.

* Basic Technology Research Center, Yokohama R&D Laboratories

2. FABRICATION OF MESFET FOR HIGH-CURRENT OPERATION

First, we fabricated a structually simple MESFET for large current operation [13~19]. Figure 1 is a schematic drawing of a GaN MESFET. A 50 nm-thick GaN buffer layer was formed on the substrate using ammonia (NH_3) as the nitrogen source and a trymethylgallium (TMG) at a low temperature, such as 873 K. An undoped 2000 nm-thick GaN layer with high resistivity was grown on a GaN buffer layer at 1323 K to obtain a high-quality GaN active layer with a thickness of 200 nm. The GaN active layer with a carrier concentration of 2.0×10^{17} cm^{-3} and a mobility of 300 cm^2/Vsec at room temperature were used to fabricate the MESFET. A 100 nm thick Si-doped layer forms the contact layer. The Si concentration of the contact layer is 2×10^{19} cm^{-3}.

The GaN was etched by a dry-etching technique using an electron cyclotron resonance (ECR) plasma to make the FET. The etching gas was a mixture of CH_4 (5 sccm), Ar (7 sccm), and H_2 (15 sccm). The microwave input power was 250 W and the DC bias voltage was 250 V. The etching rate of Si-doped and undoped GaN layers was 14 nm/min. The etching depth of GaN was about 400 nm for isolation. Furthermore, the contact layer was etched to provide the recessed gate structure. The interval of the recessed structure was 20000 nm and the etched depth was 150 nm. After patterning using a photoresist combined with a SiO_2 mask, we formed a source and a drain using Al/Ti/Au, and a Schottky gate as Pt/Au on patterned GaN samples using the ECR sputter evaporation method. The distance between the source and the drain was 30000 nm. The gate length of the GaN MESFET was 2000 nm. Source, drain, and gate electrodes of 40 unit FETs were connected using Al/Au, to obtain high-current operation. SiO_2 was used to isolate source, drain, and gate electrodes. Figure 2 is a Nomalski microphotograph of a FET connected to 40 unit FETs for high-current operation. The total gate width was 2 cm. Furthermore, four unit FETs, as shown in Figure 2, were connected by wire bonding. As a result, the total gate width was 8 cm.

Figure 3 shows the relation between the contact resistivity of ohmic electrode materials (Al/Ti/Au) and the Si concentration of the GaN contact layer. We obtained the ohmic contacts without thermal annealing. The contact resistivity was 1×10^{-6} Ωcm^2 at a Si concentration of 2×10^{19} cm^{-3}. It was thus confirmed that the contact resistivity decreased as Si concentration increased. Figure 4 shows the Schottky property between the gate and the source. The breakdown voltage was over 500 V. The maximum breakdown voltage was 600 V. The drain-source current (I_{ds}) as a function of the drain-source voltage (V_{ds}) as an FET was also obtained without cooling, as shown in Figure 5. The gate voltage (V_{gs}) was changed from 0 V to -7 V in steps of -1 V. It was found that this FET can be operated above 5 A. The on-state resistance was about 2.7 Ω. The transconductance (g_m) was about 12 mS/mm. The pinch-off voltage was about -8 V. The sheet resistivity

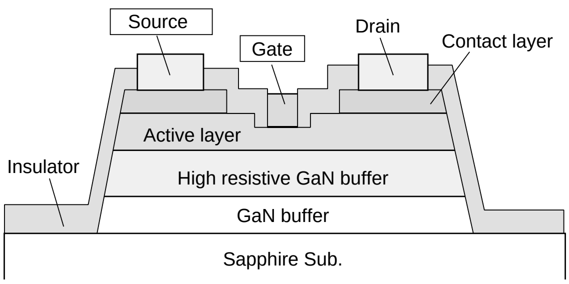

Figure 1 Schematic drawing of a GaN MESFET.

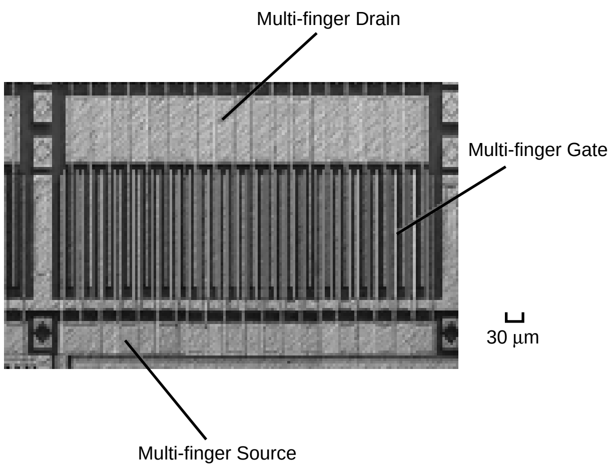

Figure 2 Nomarski micrograph of a GaN MESFET for high-current operation.

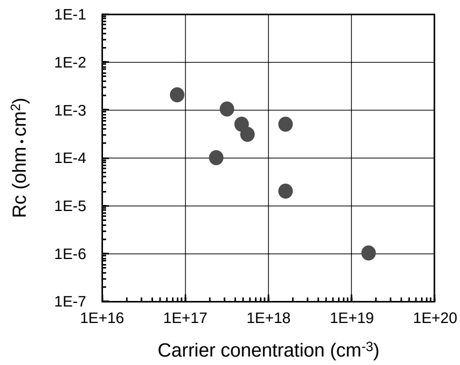

Figure 3 Ohmic contact resistivity versus carrier concentration of the GaN contact layer.

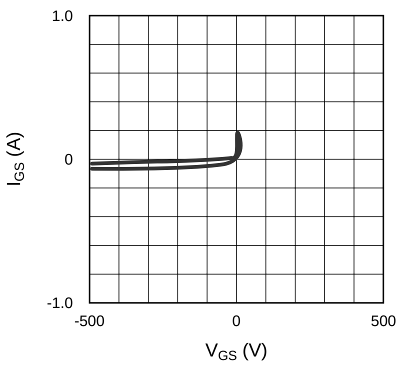

Figure 4 Schottky property between the gate and source electrodes.

of a highly resistive undoped GaN layer was about 1×10^{-6} Ω/cm^2.

To investigate whether or not electrode materials diffused into the GaN layer at 673 K, we observed the interface of the GaN MESFET using secondary ion mass spectrometry (SIMS). We also observed, using a transmission electron microscope (TEM), that the interface of the electrode materials and the GaN layer was not deformed. No degradation of the interfaces of Ti, Al, Au, and GaN layers was observed. The interfaces of the Pt, Au, and GaN layers were not deformed. Furthermore, it was confirmed that the isolating reaction of SiO_2 and electrode metal, such as Al, Ti, and Au, was not observed. Based on these results, it was confirmed that a GaN MESFET with the above-mentioned structure is effective for high-current devices.

Furthermore, we fabricated a GaN MESFET with a gate width of 20 cm and a gate length of 2000 nm. The distance between source and drain was reduced to 15000 nm. We confirmed that this FET can be operated at above 10 A by cooling it with a fan. Also, the breakdown voltage of the gate and the source was over 500 V. Based on the above-mentioned results, it was confirmed that the GaN MESFET can be operated under conditions of high current and high breakdown voltage.

3. AlGaN/GaN POWER HFET

An AlGaN/GaN heterostructure was grown using a GSMBE [18~21]. First, a Ga-rich surface was formed on a sapphire substrate surface. A 50 nm-thick GaN buffer layer was then formed on a Ga-rich surface at 973 K. A thick film of GaN was grown using Ga and ammonia gas on the GaN buffer layer at 1073 K. An $Al_{0.2}Ga_{0.8}N$/GaN heterostructure was also grown using ammonia gas at 1073 K. The thickness of undoped $Al_{0.2}Ga_{0.8}N$ was 30 nm and that of undoped GaN was 2000 nm.

Next, we fabricated an HFET having the schematic structure shown in Figure 6. The GaN and $Al_{0.2}Ga_{0.8}N$ were etched using a dry-etching technique with an ECR plasma to make the FET. The etching gas was a mixture of CH_4 (5 sccm), Ar (7 sccm) and H_2 (15 sccm). The etching rate of GaN layers was 14 nm/min. The etching depth of GaN was about 400 nm for isolation. Furthermore, the contact layer of a Si-doped GaN layer with a carrier concentration of 5×10^{19} cm^{-3} was selectively grown in the region of the source and the drain. After patterning using a photoresist combined with a SiO_2 mask, we formed a source and a drain using Al/Ti/Au, and a Schottky gate as Pt/Au on a patterned GaN sample using an ECR sputter evaporation method. Figure 7 shows a schematic cross-sectional drawing of AlGaN/GaN HFET for high-current operation. The distance between the source and the drain was 6000 nm. The gate length was 2000 nm. Source, drain, and gate electrodes of 400-unit FETs were connected using Al/Au, respectively, to obtain high-current operation. SiO_2 was used to isolate source, drain, and gate electrodes. The total gate width was 20 cm. The area of the FET was about 0.15 cm^2.

The Hall mobility of the AlGaN/GaN layer was about 1200 cm^2/Vs and the sheet carrier density was 1×10^{13} cm^{-2} at room temperature. We investigated the relation between contact resistance and carrier concentration of the contact layer. Ohmic contacts were obtained under conditions without thermal annealing. The lowest contact

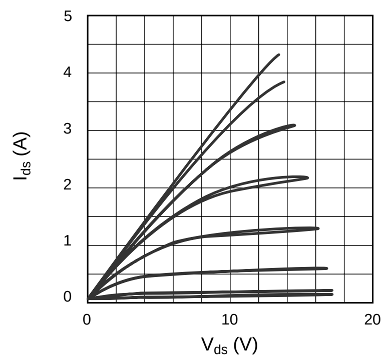

Figure 5 Current-voltage characteristics (I_{ds}-V_{ds}) of a GaN MESFET with a gate width of 8 cm. The gate voltages were changed from 0V to -8 V in steps of -1 V.

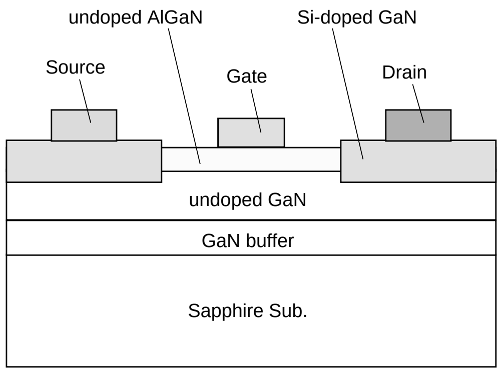

Figure 6 Schematic drawing of an AlGaN/GaN HFET.

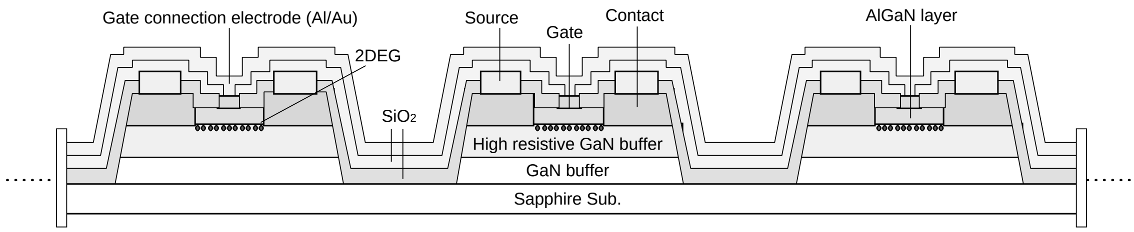

Figure 7 Schematic cross-sectional drawing of AlGaN/GaN power HFET.

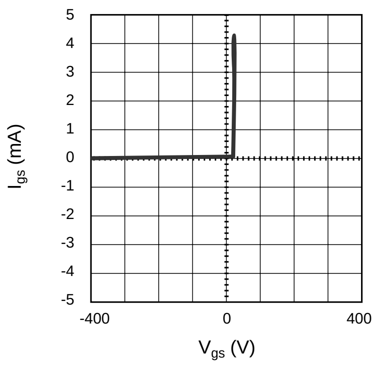

Figure 8 Schottky property of gate and source of an AlGaN/GaN HFET.

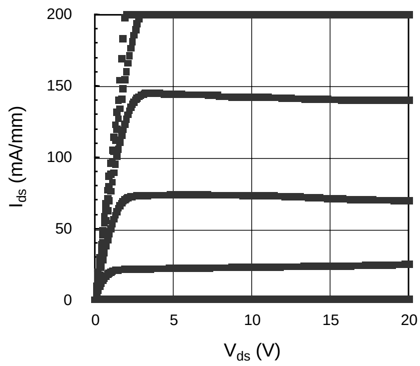

Figure 9 Current-voltage property of a unit AlGaN/GaN HFET at room temperature. The gate voltage (V_{gs}) was changed from 0 V to -5 V in steps of -1 V.

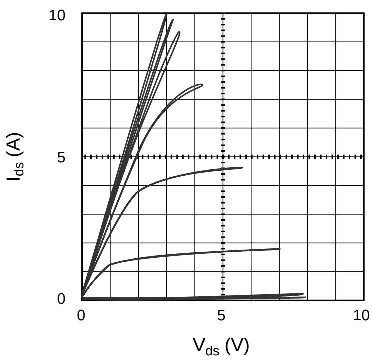

Figure 10 Current-voltage property of an AlGaN/GaN HFET under high- current operation. The gate voltage (V_{gs}) was changed from 0 V to -7 V.

resistance was 3.5×10^{-8} Ωcm^2 at a carrier concentration of 5×10^{19} cm^{-3}. We also investigated the breakdown voltage of a highly resistive undoped GaN layer by removing the AlGaN layer, because a highly resistive layer is important for the high breakdown voltage of an FET. Electrodes with a 10000 nm gap were fabricated on the undoped GaN buffer layer. It was also confirmed that an undoped GaN layer had a high breakdown voltage above 2000 V. The breakdown field of an undoped GaN layer was estimated to be 2.0 MV/cm. Figure 8 shows a Schottky property between the gate and the source. The breakdown voltage was over 550 V. The maximum breakdown voltage was 600 V. We observed through a secondary electron microscope (SEM) that the AlGaN/GaN layer was not damaged after supplying 600 V, although only the Shottky electrode was broken by a high electric field. That is, the AlGaN/GaN layer had sufficient strength for a high voltage. It is expected that the breakdown voltage will be further increased by improving electrode materials.

Figure 9 shows the current-voltage property of a one-unit AlGaN/GaN HFET. The drain-source current (I_{ds}) was measured in the range from 0 mA to 100 mA. The gate voltage (V_{gs}) was changed from 0 V to -5 V in steps of -1 V. The pinch-off voltage was about -5 V. In our measurement system, we could not observe the current to 100 mA, because the current limit was 100 mA. We also measured with a curve-tracer that the saturation current (I_{ds}) at V_{gs} = 0 V was 330 mA/mm. The maximum transeconductance (g_m) was about 120 mS/mm. This property was very stable. This FET was also operated above 100 V of the drain-source voltage (V_{ds}). The specific on-state resistance (R_{on}) was estimated to be about 2 $m\Omega cm^2$. This R_{on} was lower than that of Si devices [21]. The specific on-resistance of Si-MOSFET was about 10 $m\Omega cm^2$ at a breakdown voltage of 100 V. It was confirmed that the specific on-resistance of an AlGaN/GaN HFET was lower than that of a Si MOSFET.

To measure the high-current operation of the AlGaN/GaN HFET, we carried out wire-bonding for the HFET. Figure 10 shows the I_{ds}-V_{ds} property of the HFET. The HFET was operated above an I_{ds} of 10 A. The maximum Ids was about 20 A. This was the highest of the previously reported values [20]. The on-state resistance for high-current operation was 40 $m\Omega cm^2$, and the breakdown voltage was 100 V. The on-state resistance of this FET is slightly higher than that of a unit FET. This is why all 400-unit FETs were not completely operated due to surface defects in the epitaxial wafer and the fabrication accuracy of the FET. This problem can be solved by improving the epitaxial wafer and the accuracy of the fabrication process. Based on these results, it was confirmed that an AlGaN/GaN HFET with the above-mentioned structure is effective for large-current devices. This HFET is very promising for low-loss power switching devices such as inverters or converters.

4. SUMMARY

A high-power AlGaN/GaN HFET for high-current operation was fabricated for the first time. An AlGaN/GaN heterostructure was grown by GSMBE. The total gate width of the HFET was 20 cm and the gate length was 2000 nm. Gate, source, and drain were isolated using SiO_2. The distance between the source and the drain was 6000 nm. The electrode materials of the source and the drain were Al/Ti/Au, and the Schottky electrodes were Pt/Au. The maximum breakdown voltage of gate and source was 600 V. An undoped GaN layer had a high breakdown voltage above 2000 V and the breakdown field of the undoped

GaN layer was 2 MV/cm. The on-state resistance of a unit HFET was 2 mΩcm^2. The maximum operation current of an HFET with a 20 cm in gate width was 20 A. An HFET for high-current operation was thus demonstrated. GaN based FETs are therefore excellent for low-loss power switching devices.

REFERENCES

1) S. Yoshida: Journal of Applied Physics of Japan 68, 787 (1999). (in Japanese)
2) E. O. Johnson: RCA Rev. 26, 163 (1965).
3) R. W. Keys: Proc. IEEE, 60, 225, (1972).
4) B. J. Baliga: IEEE Electron Device Lett. 10, 455, (1989).
5) B. J. Baliga: J. Appl. Phys., 53, 1759, (1982).
6) K. Shenai, R. S. Scott, and B. J. Baliga: IEEE Trans. Electron Devices, 36, 1811, (1989).
7) T. P. Chow and R. Tyagi: IEEE Trans. Electron Devices, 41, 1481, (1994).
8) S. C. Binari, K. Doverspike, G. Kelner, H. B. Dietrich, and A. E. Wickenden: Solid State Electron. 41, 97 (1997).
9) S. Yoshida and J. Suzuki: Jpn. J. Appl. Phys. Lett. 37, L482 (1998).
10) S. Yoshida and J. Suzuki: J. Appl. Phys. 84, 2940 (1998).
11) M. A. Khan, M. S. Shur, J. N. Kuzunia, Q. Chin, J. Burm, and W. Schaff, Appl. Phys. Lett. 66, 1083 (1995).
12) A. Oezuer, W. Kim, Z. Fan, A. Botchkarev, A. Salvador, S. N. Mohammad, B. Sverdlov, H. Morkoc: Electron. Lett. 31, 1389 (1995).
13) S. Yoshida, M. Sasaki, and H. Kawanishi: J. Cryst. Growth 136, 37 (1994).
14) S. Yoshida and M. Sasaki, Appl. Surf. Sci. 82/83, 28 (1995).
15) S. Yoshida: J. Appl. Phys. 81, 7966 (1997).
16) S. Yoshida: J. Cryst. Growth, 181, 293 (1997).
17) S. Yoshida: J. Cryst. Growth, 191, 279 (1997).
18) S. Yoshida and J. Suzuki, J. Appl. Phys, 85, 7931 (1999).
19) S. Yoshida and H. Ishii, Proc. Mat. Res. Soc., (2001) G13.4.
20) S. Yoshida and H. Ishii, to be published in Physica Status Solidi (B) (2001).
21) S. Yoshida and H. Ishii, to be published in Proc. ICSCRM (2001).

Manuscript received on November 22, 2001.